

Two-Dimensional Nucleation with Edge and Corner Diffusion

Yukio Saito

Department of Physics, Keio University, 3-14-1 Hiyoshi, Kohoku-ku, Yokohama 223-8522, Japan
(Dated: May 21, 2019)

The effect of edge and corner diffusions on the morphology and on the density of islands nucleated irreversibly on a flat substrate surface is studied. According to the strength of the edge and the corner diffusion constants, D_e and D_c , relative to the surface one D_s , we observe square, diamond, cross, regular and irregular dendritic shapes. Without or with weak corner diffusion, the critical island size is $i_c = 1$, and the island density n at the deposition rate F satisfies the scaling relation $n / (D_s F)^{1/3}$, irrespective of the island morphology. With a large corner diffusion constant, on the other hand, the density of square islands decreases and satisfies another scaling relation $n / (D_c D_s F^2)^{2/9}$. The latter is found to be due to the possibility of migration of small clusters $i \leq 3$. The size distribution also differs in two cases.

PACS numbers: 68.55.-a, 68.43.Jk, 05.70.Ln, 81.10.Aj

I. INTRODUCTION

Surface morphology during epitaxial growth depends on processes taking place on the substrate.^{1,2,3,4,5,6} At very low temperatures as in the case of molecular beam epitaxy (MBE), deposited atoms are adsorbed and migrate on the substrate surface until they form nuclei or are incorporated into islands, but they never evaporate back to the ambience. When an adsorbed atom (adatom, for short) sticks and freezes irreversibly to an island, the resulting aggregate takes an irregular dendritic shape,^{1,2,6} called diffusion-limited aggregate (DLA).⁷ It has a characteristic feature of self-similarity, and is regarded as a typical example of a fractal. In actual experiments, one does not always observe fractal but also compact islands.^{2,3} Compact islands are possible when atoms on the step edge of the island can detach from it⁸ or diffuse along it.^{9,10,11,12} Since at low temperatures it is difficult for an edge atom to detach, the edge diffusion mainly governs the island morphology. During the edge diffusion, however, the outer corner provides an additional barrier to be surpassed. There, an edge atom has to pass an intermediate state where the number of neighboring bonds is less than that on the straight step edge. The edge and the corner diffusion is known to influence the island morphology.^{9,10,11} Furthermore, the corner diffusion barrier is found to induce mound formation for multilayer deposition.^{13,14}

For the submonolayer deposition, the density of nucleated islands is known to depend on the rate of the surface diffusion constant and the deposition rate.^{15,16} When the deposition rate F is large, the adatom density is high and the nucleation occurs frequently. Thus the island density is expected to be high. For a large surface diffusion constant D_s , on the other hand, the deposited atoms will move around a long distance until they find nucleation partners or preexisting islands and stick to them. Thus, the rate of forming new nuclei is low, and the island density on a singular surface should decrease as the diffusion rate increases. By assuming that the island is a point sink to diffusing adatoms and the criti-

cal nuclear size is $i_c = 1$, the island density is expected to be proportional to $(F/D_s)^{1/3}$.^{15,16,17} This prediction is confirmed by the kinetic Monte Carlo (KMC) simulation with point islands.¹⁷ Actual islands increase their size during deposition, and the scaling relation between the density and the diffusion constant might depend on the island morphology. There are already many studies on the island density by means of KMC simulation,^{9,18} but we study here the relation between the island density and the morphology obtained with various combinations of the surface, edge and corner diffusion processes, systematically.

In Sec. II, we explain our simulation scheme. In Sec. III, the island morphology is found to depend strongly on the edge and corner diffusion constants. Without them, islands are similar to DLA, with edge diffusion they take cross shapes, with corner diffusion in addition they become square. The island density is discussed in Sec. IV. As long as the corner diffusion is small, the density scaling is found independent of the island morphology with an exponent $1/3$. With a large corner diffusion constant, small islands of sizes less than 3 ($i \leq 3$) can migrate on the surface, and the coarsening takes place. The island density becomes low with a rather narrow island size distribution, and the density scaling changes with another exponent $4/9$. The result is summarized and discussed in the last Sec. V.

II. MONTE CARLO SIMULATIONS

Our main aim is to explore the systematics and the universal features of the morphology change of islands on a singular surface as the diffusion mechanism changes, rather than the precise reproduction of experimentally observed island shapes. For this purpose, we adopt the simplest model such that atoms are depositing on a (100) surface of a simple cubic lattice with a solid-on-solid (SOS) restriction. The SOS restriction is valid at low temperatures, common to MBE.

Atoms are deposited randomly onto the substrate with

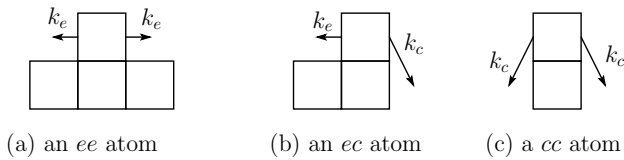


FIG. 1: Diffusion processes of an adatom connected to an island with a single in-layer bond. k_e is the rate of edge diffusion and k_c is that of corner diffusion.

a deposition rate of F monolayers per unit time. Here we choose the unit of time such that $F = 1$. The temperature is assumed to be so low that all deposited atoms stick to the surface and never evaporate back into the ambient. An isolated adatom hops to one of its four nearest neighboring sites at a rate k_s ; the waiting time of an adatom before the jump is $(4k_s)^{-1}$, and the surface diffusion constant is given by $D_s = k_s a^2$, where a is the lattice constant. As for the interlayer diffusion, which takes place in case a deposited atom lands on another adatom, no additional energy barrier is assumed. On the contrary, atoms at the edge are not allowed to hop up a layer. Therefore, Ehrlich-Schwobel mound formation is suppressed, and the layer-by-layer growth is expected.

When an atom touches to other adatoms or islands, it makes a nearest neighbor bond to form a cluster. At very low temperatures corresponding to the MBE, this cluster will never dissociate again. Atoms attach clusters irreversibly. This means that dimers are stable and will not break up, and the critical island size is $i_c = 1$. Nevertheless, if an edge atom is singly-bonded in the layer, i.e. if it makes only one bond with another adatom, it is possible to diffuse along the island periphery at moderate temperatures. There are two possible diffusion jumps for a singly-bonded atom; an edge diffusion along the straight step edge, and a corner diffusion across the outer corner. The rate of edge diffusion is k_e and that of corner is k_c , as is depicted in Fig.1. Then, a singly-bonded atom can be classified by its possible motions in two directions. It is classified as (a) an ee atom on the straight step if both motions are along the step edge, (b) an ec atom at the ridge of corner if one is the edge diffusion and the other is the corner, and (c) a cc atom on the tip if both motions are across the corner, as shown in Fig.1. The edge diffusion constant along the straight step edge is $D_e = k_e a^2$, and we may define the corner diffusion constant as $D_c = k_c a^2$. Precise values of diffusion constants depend on the energy barriers and the temperature. For edge and corner diffusion there may exist extra energy barriers in addition to that for the surface diffusion, and diffusion constants are probably ordered as $D_s \geq D_e \geq D_c \geq 0$. If an edge atom is incorporated into the kink site with more than two nearest neighbors, it ceases migration, for simplicity.

Simulation starts from a clean substrate surface of a size $L_x \times L_y$ without adatoms. Hereafter we take the lattice constant $a = 1$. Therefore, the jump rates k 's and

diffusion constants D 's are the same. During the simulation, at some stage, there are N_0 isolated adatoms, N_{ee} edge atoms attached to a straight step edge, N_{ec} atoms at the corner, and N_{cc} atoms at the tip position (see Fig.1) on the surface. These adatoms are sorted out in corresponding lists. The transition probability from this configuration to the next one is given as follows. The rate of the deposition is $P_d = FL^2$, of the surface diffusion $P_s = 4N_0D_s$, of the edge diffusion $P_e = (2N_{ee} + N_{ec})D_e$ and of the corner diffusion $P_c = (N_{ec} + 2N_{cc})D_c$. The total probability of state change in a unit of time is $P_t = P_d + P_s + P_e + P_c$. Thus, within a time interval $dt = 1/P_t$, one of the events takes place; the deposition with a probability $P_d dt$, the surface diffusion with $P_s dt$, the edge diffusion with $P_e dt$ and the corner diffusion with $P_c dt$. For each diffusion process, the atom to be moved is picked up from the list. After each state change, adatom lists have to be adjusted, for example, by eliminating those adatoms with more than two neighboring bonds from the lists. The time is incremented by dt . The monolayer is covered at a time $t = 1$, in principle, but because of the stochastic feature of the simulation algorithm, actual time for the completion of a monolayer fluctuates around $t = 1$:

III. ISLAND MORPHOLOGY

Simulations are performed for systems of sizes 100, 100, 200, 200, and 1000, 1000 under various combinations of diffusion constants, and some typical island morphology is shown in Fig.2 at a coverage of 0.1 monolayer (ML).

From Fig.2 (a) to (e) the edge and corner diffusion constants, D_e and D_c , are equally increased from 0 to D_s , by keeping the surface diffusion constant D_s fixed at $D_s = F = 10^9$. Without diffusion along the edge of an island, it takes an irregular dendritic form or a fractal DLA-like shape, as shown in Fig.2 (a). On increasing the edge and corner diffusion to $D_e = D_c = 10^6 D_s$, dendrite branches thicken and they extend mainly in $[11]$ direction, as shown in Fig.2 (b). Further increase of $D_e = D_c = 10^5 D_s$ let the islands compact in hopper shapes, as in Fig.2 (c). At $D_e = D_c = 10^4 D_s$, islands take square shape with rather straight flog steps, as in Fig.2 (d). When all the diffusion constants are equal, as in Fig.2 (e), islands are square and very large, but their density decreases dramatically. On this density change we shall discuss later in Sec.IV. The sequence of simulations from Fig.2 (b) to (d) almost corresponds to the parameter range studied by Bales and Chrzan⁹ by changing the temperature. The morphology variation is of course quite analogous to what they have obtained.

We now study the effect of corner diffusion more precisely, in a sequence of pictures shown from Fig.2 (e) to (i). There, the surface and the edge diffusion constants are kept equal, $D_e = D_s$, and only the corner diffusion constant D_c is decreased from D_s to 0. In all these cases,

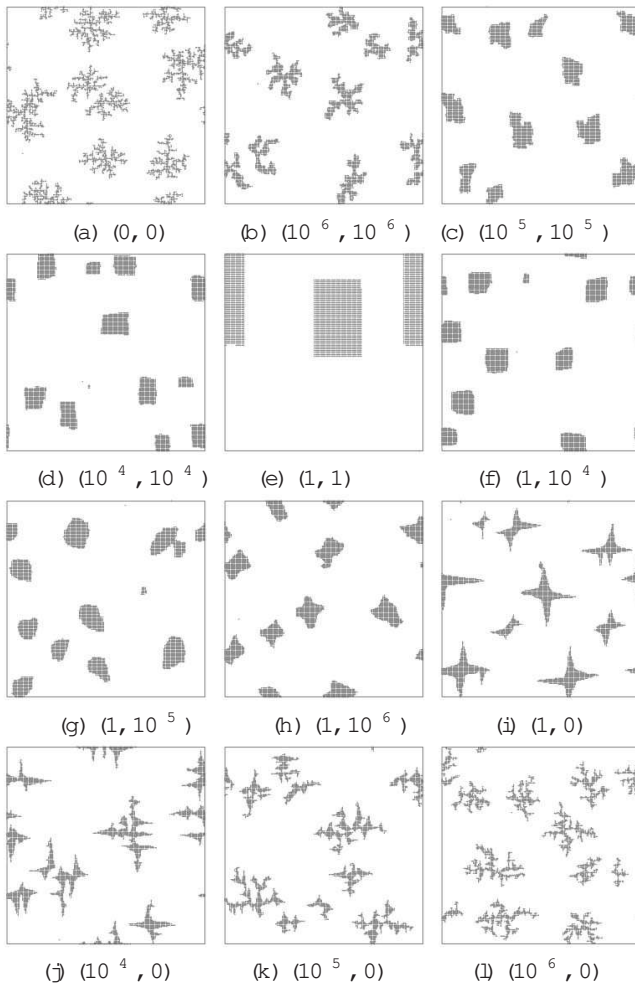


FIG. 2: Island morphology at various combinations of the surface, edge and corner diffusion constants, D_s, D_e and D_c . D_s is fixed at $D_s = F = 10^9$. Parameters in parentheses represent $(D_e = D_s; D_c = D_s)$. The system size is 200×200 , and the coverage is $\theta = 0.1ML$.

islands are found compact. With a large corner diffusion constant, $D_c = 10^4 D_s$, islands are square with 10^6 steps, as shown in Fig. 2 (e) and (f). At $D_c = 10^5 D_s$ in Fig. 2 (g), they look round and rather isotropic, and for a still smaller $D_c = 10^6 D_s$ in Fig. 2 (h) some islands look diamonds and some others crosses with thick arms. In the extreme case of Fig. 2 (i) without the corner diffusion, $D_c = 0$, islands consist four sharp needles growing in the $[10]$ direction.

In a series of simulations (i)–(l) the corner diffusion is completely suppressed ($D_c = 0$), and the effect of the edge diffusion D_e is exemplified. The series, in fact, continues back to (a). With $D_e = D_s$ in (i) needles of each cross-shape island are rather stable and sidebranches are rare. On decrement of edge diffusion to $D_e = 10^4 D_s$ in (j), needles have many sidebranches growing in $[10]$ direction. Further decrement of $D_e = 10^5 D_s$ leads to tip splitting in Fig. 2 (k). With still smaller $D_e = 10^6 D_s$ clusters look like DLA aggregates. Comparison with

Fig. 2 (b) and (l) reveals that the corner diffusion produces $[11]$ dendrite in Fig. 2 (b), whereas without corner diffusion aggregates have a preference in $[10]$ direction in Fig. 2 (l).

From these variety of island morphology the edge and corner diffusions are found to play different roles. The edge diffusion smears out shot noise introduced by the irreversible attachment, and permits the formation of compact islands. The corner diffusion varies the orientational preference. Without the corner diffusion, those atoms on the tip positions or on the narrow step edges cannot cross to the other sides of an island, and thus the supersaturation on the narrow $[10]$ side increases. This leads to the enhancement in the growth velocity normal to the narrow $[10]$ side, and eventually the dendritic tips are formed into $[10]$ direction due to this strongly anisotropic kinetic effect. Similar instability of a straight step in $[10]$ orientations is observed in previous simulations,^{13,14} and the instability is shown to change the island morphology here. This instability is expected to induce mound formation for multilayer adsorption even without the diffusion bias or the Ehrlich-Schwoebel effect. That is a future problem to be studied. With a corner diffusion, islands try to be square. If the edge diffusion is weak, however, the adatom supply at the center of the step edge is insufficient, and the corner instability takes place. This leads to the dendrite growth in the diagonal $[11]$ direction.

IV. ISLAND DENSITY

In Fig. 2 at a fixed surface diffusion constant D_s , we observe that the island density is almost independent of the edge and corner diffusion constants, D_e and D_c . We said "almost", because in Fig. 2 (e) the island density is clearly different from the others. We now study the effect of peripheral diffusion on the island density.

The rate equation analysis predicts that the island density n depends on the surface diffusion constant D_s as $(F = D_s = F)^{-i} = (i + 2)^{-1}$ when the critical island size is i .^{15,16} Simulations where the temperature is varied is inappropriate for a systematic study on the effect of edge and corner diffusion, since the critical island size i varies as well. To study the relation of island morphology and its density by fixing $i = 1$, we control directly on the rate of edge and corner diffusion, rather than tune many parameters as bond energies, energy barriers and the temperature.

The island density n at 10 percent of monolayer coverage is plotted in Fig. 3 as a function of the surface diffusion constant $D_s = F$ for various combinations of the edge and corner diffusion constants. The system sizes plotted are 200^2 (open circles) and 1000^2 (filled circles).

For the case without edge and corner diffusion, $D_e = D_c = 0$, islands are fractal as shown in Fig. 2 (a), at least at low densities with a large D_s . The island density is shown in Fig. 3 (b). Data fits well with the scaling relation $n = 0.23(D_s = F)^{-1.3}$. There, another scaling law

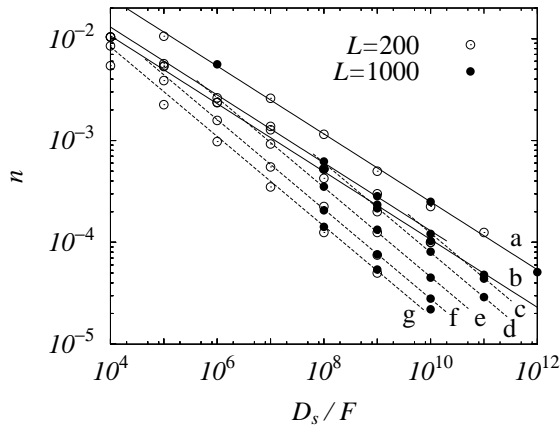


FIG. 3: Both logarithmic plot of the island density n at the coverage $\theta = 0.1M L$ versus the surface diffusion constant normalized by the deposition rate D_s/F . The values of edge and corner diffusion constants, D_e and D_c , are (a) $D_e = D_s$ and $D_c = 0$ (no corner diffusion), (b) $D_e = D_c = 0$ (without edge and corner diffusion), (c) $D_e = D_c = 10^4 D_s$, (d) $D_e = D_c = 10^3 D_s$, (e) $D_e = D_c = 10^2 D_s$, (f) $D_e = D_c = 10^1 D_s$, and (g) $D_e = D_c = D_s$. In (a) the horizontal axis is displaced to the right by a factor 10, for visual reason. Lines represent scaling behaviors as $n \propto (D_s/F)^{-\beta}$. An exponent for straight lines is $\beta = 1/3$, and for dashed lines $\beta = 0.44$.

$n \propto (D_s/F)^{-2/(4+D_f)}$ is proposed, where $D_f = 1.71$ is the fractal dimension of the DLA.^{19,20} From the present simulations of sizes up to 1000^2 , we cannot discriminate which of the two scaling laws is superior.

For the case with a large edge diffusion $D_e = D_s$ but without corner diffusion $D_c = 0$, islands have cross shapes as in Fig.2 (i). Even for this situation, the density n is compatible with a scaling law $n \propto 0.25 (D_s/F)^{-1/3}$, as is shown in Fig.3 (a). The plot is shifted by a factor 10 to the right for the visual purpose. Otherwise, data overlaps almost completely with those for fractal islands, Fig.3 (b).

With or without edge diffusion, the island density is found to follow the same scaling relation with the surface diffusion constant D_s/F , obtained by a simple rate equation theory.^{15,16} Inclusion of the corner diffusion, however, drastically changes the situation. By keeping $D_e = D_c$ but at different ratio to the surface diffusion as (c) $D_e = D_s = D_c = 10^4$, (d) 10^3 , (e) 10^2 , (f) 10^1 , and (g) 1, the relation between the island density n and the surface diffusion constant D_s/F varies as shown in Fig.3 (c)-(g). For (c) the island density at low $D_s/F = 10^{10}$ is higher than that (b) of fractal islands by about 20 percent, $n \propto 0.28 (D_s/F)^{-1/3}$. This density increase is due to the compactness of the islands, as shown in Fig.4 (b), compared to the fractal islands in Fig.4 (a). There are more space for adatoms to nucleate new islands. As for the D_s dependence, the island density follows the same scaling law with a power $1/3$, unless D_s

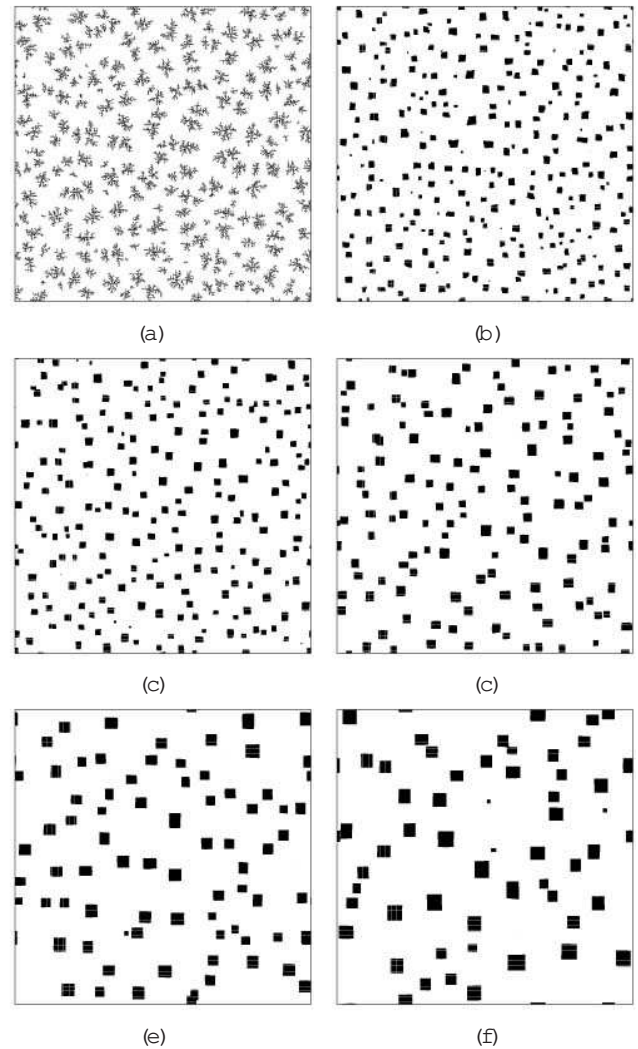


FIG. 4: Islands on a substrate of a size 1000^2 at a coverage $\theta = 0.1M L$. $D_s/F = 10^9$ and $D_e = D_c$. The ratio of the corner to surface diffusion constant D_c/D_s is (a) 0, (b) 10^4 , (c) 10^3 , (d) 10^2 , (e) 10^1 , and (f) 1.

takes the largest value $D_s/F = 10^{11}$. There, the density becomes less than that of fractal islands, Fig.3 (b).

As D_e and D_c increase further from Fig.3 (d) to (g), the island density starts to deviate from the curve (c) at smaller D_s/F . For the case (d) with $D_e = D_s = D_c = 10^3$, deviation takes place at about $D_s/F = 10^9$, for (e) at about $D_s/F = 10^7$. For (f) and (g) with larger $D_e = D_c$, the island density remains always less than that of fractal islands with the same D_s . This tendency of density decrease is obvious by plotting the surface configurations in Fig.4. There, the coverage $\theta = 0.1M L$ and the surface diffusion constant $D_s/F = 10^9$ are the same, but the edge and corner diffusion constants, $D_e = D_s = D_c = D_s$, are varied. On increasing D_c from Fig.4 (c) to (f), the number of islands decreases and the island size increases.

From (c) to (g), the island density n seems to satisfy

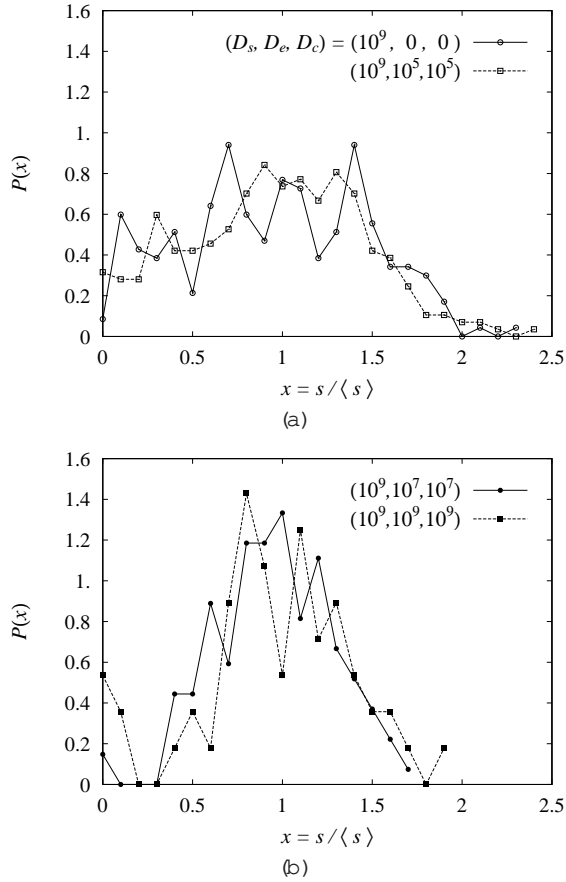


FIG. 5: Island size distribution with (a) low and (b) high corner diffusion constant, D_c .

a new scaling relation with the surface diffusion constant $D_s = F$ with an exponent $\nu = 0.44$ (depicted by dashed lines in Fig.3), when the density n is lower than that of fractal islands. At (g) when all the surface, edge and corner diffusion constants are equal, the island density can be fitted to another exponent $\nu = 0.41$. But there the density is very low, especially at $D_s = F = 10^{10}$, and the data is not much reliable. Therefore, we rather draw the line with the same exponent $\nu = 0.44$ in Fig.3.

From Fig.4, one further notices that as the corner diffusion constant D_c increases, not only the total number of islands but also the island size distribution changes. This tendency is apparent by plotting island size distribution in Fig.5. Among $N_i = nL^2$ islands, there are $N(s)$ islands of a size s . Since the average island size $\langle s \rangle$ changes as D_c varies, the distribution of islands with a normalized size $x = s/\langle s \rangle$ has the relevant concern. We define the probability $P(x) = x$ as the number of islands with sizes between x and $x + \Delta x$ divided by the total number of islands N_i with $\Delta x = 0.1$. At low D_c 's as $D_c = 0$ and $10^4 D_s$ in Fig.5(a), the island sizes are widely spread and almost constant for sizes up to 1.5 times the average size $\langle s \rangle$. This is the typical size distri-

bution for fractal islands, without special size, other than the islands separation in the present case. There are also a few very large islands with sizes about 2.5 times the average size. On the contrary, at high D_c 's the island size distribution has a narrow peak around the average size. There is a gap at small islands density, and the distribution extends less than twice the average size in the region of large sizes. The difference in the island density scaling should be related to this absence of small-sized islands at high D_c .

V. DISCUSSIONS AND CONCLUSIONS

We have seen that the corner diffusion influences the island density and the size distribution drastically. Without or weak corner diffusion, the island density varies in proportion to D_s with a power $1/3$, irrespective of the island morphology. This means that the nuclei are formed at the initial stage of deposition, as soon as the two adatoms collide each other. They are immobile and act as a center of nucleation. Therefore, the randomness of the two-adatom encounter is frozen in. After sufficient density of nuclei is formed, further deposited adatoms are incorporated into the preexisting clusters. They develop into various shapes, depending on the edge and corner diffusion constants. Since the nucleation takes place at random, the island sizes are distributed rather homogeneous, reflecting the randomness in the island separation. In any case, this scenario permits the island density to be independent of the morphology: The island density is determined long before the island shape appears.

With a large corner diffusion, on the other hand, inspections of the time evolution reveal that clusters of small sizes $i = 3$ are still mobile. Since two or three adatoms can move around each other via the corner diffusion, small clusters migrate around randomly on the substrate surface. During this cluster diffusion, they coagulate with isolated atoms and as a result the island density decreases. Only when compact islands as squares with more than doubly bonded atoms is formed, it ceases migration on the substrate surface, and starts to act as a nucleation center. During the further stage of cluster growth, the adsorbed atoms form small mobile clusters and are incorporated into islands in group. This alters the situation assumed in the rate equation theory.^{15,16} There the monomer incorporation is assumed for the island size increase and predicts the island density n to be proportional to $(D_s = F)^{i-1} = (i+2)$ with the critical island size i . For $i = 3$, it predicts a scaling exponent 0.6, quite different from the obtained value 0.44.

For small clusters to migrate on the substrate surface, an adatom in the cluster has to pass two outer corners in the same direction. Therefore, the waiting time τ_c for a center of mass of a small cluster to make a random jump is proportional to $k_c^{-2} D_c^{-2}$. When the jump rate τ_c^{-1} is larger than the frequency of an isolated adatom migration $\tau_a^{-1} = k_s D_s$, new mechanism for

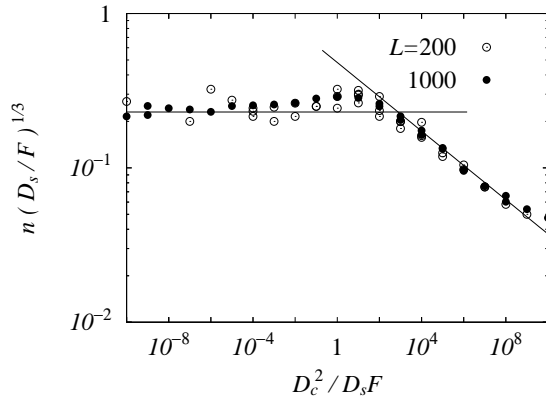


FIG. 6: The scaled island density $n(D_s=F)^{1/3}$ as a function of the scaled corner diffusion constant $D_c^2/D_s F$. Horizontal line is $n(D_s=F)^{1/3} = 0.23$, and the inclined line represents the relation $n(D_s=F)^{1/3} / (D_c^2/D_s F)^{1/9}$.

the island density scaling may set in. To highlight the crossover between two different scaling behaviors, the island density n is multiplied by $(D_s=F)^{1/3}$, and the product is plotted against the ratio of the two waiting times or $D_c^2/D_s F$ ($a=c$) in Fig.6. There, diffusion constants span wide ranges as $D_s=F = 10^5 - 10^{11}$ and $D_c = D_e = 10^{10} D_s - D_s$. Many data points collapse on a universal curve quite well. With small corner diffusion constants, the density stays close to the values expected from the scaling law $n = A(D_s=F)^{1/3}$, where the coefficient $A = 0.23$ for $D_e = D_c = 0$ is shown by a horizontal line in Fig.6. There is a weak dependence of the coefficient A on D_c and on D_e . It is attributed to the compactness change of islands for finite D_e and D_c . When D_c^2 gets closer to D_s , small clusters start to migrate on the substrate and the scaling behavior changes. The inclined line in Fig.6 represents the scaling $n(D_s=F)^{1/3} / (D_c^2/D_s F)^{1/9}$. So far, we have no explanation of the new exponent around $1/9$.

According to the rate equation analysis by Villain et al.¹⁹ the dimer diffusion leads to the island density n in proportion to $(D_s D_2 = F^2)^{1/5}$, where D_2 is the dimer diffusion constant. The exponent 0.4 for the F -dependence is quite close to our estimation ≈ 0.44 in Fig.3. As for the dependence on diffusion constants, one has to know D_2 in terms of our model parameters. Since dimer dissociation is prohibited, the dimer diffusion is possible only by corner diffusion, and D_2 should be a function of D_c . When we assume that n in Fig.3 actually follows the scaling $n(D_s=F)^{2/5} (D_c=D_s)$ for large D_s and for fixed ratio of $D_c=D_s$, the D_s dependence of the rate equation theory leads to $\approx 1/5$ and D_2/D_c . Then, a normalized island density $n(D_s=F)^{1/3}$ should indicate a universal behavior in terms of $D_c^3/D_s F$. If, on the other hand, one

uses the relation $D_2 = D_c^2$ as we have adopted in Fig.6, the normalized density $n(D_s=F)^{1/3} / (D_c^3/D_s F)^{1/3}$ should show a universal behavior in terms of $D_c^3/D_s F$. Both the above scaling plots fail in data collapse on a universal curve, as is accomplished in Fig.6. In fact, there are differences in our situation from the assumptions in the rate equation theory.¹⁹ Our dimers never dissociate, and the trimers as well as dimers migrate at large D_c . These differences might modify the precise form of the island density scaling.

We now summarize our study of the edge and corner diffusion effect on the morphology and on the density of islands, which are nucleated irreversibly on a flat substrate surface at a submonolayer coverage. With only the surface diffusion, the irreversibly nucleated islands have a fractal shape characteristic to DLA. With the edge diffusion, islands become thick and compact. The corner diffusion affects the shape anisotropy. One may typically say that without the corner diffusion dendrites pointing in $[10]$ direction appear, whereas with it squares with $[10]$ faces appear.

The density of islands is mainly determined before the shape appears. Without or with a weak corner diffusion, the critical island size is $i = 1$, and the density n is related to the surface diffusion constant D_s normalized by the deposition rate F as $n / (D_s=F)^{1/3}$, irrespective of island morphology. With a large corner diffusion constant, on the other hand, small clusters $i = 3$ can migrate randomly on the substrate surface, and another scaling relation $n / (D_c D_s = F^2)^{2/9}$ is found. As far as we know, explanation to the latter scaling law is still lacking. The whole scaling behavior is well described by a universal form, $n = (D_s=F)^{1/3} f(D_c^2/D_s F)$. The function $f(x)$ approaches to a constant value for small x , and to $x^{-1/9}$ for large x .

Recently, the mobility of large clusters is proposed to be very effective in selecting the island size and in ordering the mutual arrangement in heteroepitaxial growth.²¹ Our model allows the motion of only small clusters less than the size $i = 3$ by the corner diffusion, and some size selection is observed. Due to the absence of any direct interaction between islands, however, the ordering in island positions cannot be achieved. Our model neither contains the size-limiting effect, and the coarsening takes place as the corner diffusion increases.

Acknowledgments

This work is supported by Grant-in-Aid for Scientific Research from Japan Society of the Promotion of Science. The author is benefited from the inter-university cooperative research program of the Institute for Materials Research, Tohoku University.

Electronic address: yukio@rk.phys.keio.ac.jp

- ¹ R. Q. Hwang, J. Schroder, C. Gunther, and R. J. Behm, *Phys. Rev. Lett.* **67**, 3279 (1991).
- ² T. Michely, M. Hohage, M. Bott, and G. Comsa, *Phys. Rev. Lett.* **70**, 3943 (1993).
- ³ J. A. Strosio, D. T. Pierce, and R. A. D'ragoet, *Phys. Rev. Lett.* **70**, 3615 (1993).
- ⁴ H. Brune, C. Romainszyk, H. Roder, and K. Kem, *Nature (London)* **369**, 469 (1994).
- ⁵ H. Brune, C. Romainszyk, H. Roder, and K. Kem, *Appl. Phys. A* **60**, 167 (1995).
- ⁶ M. Hohage, M. Bott, M. Morgenstern, Z. Zhang, T. Michely, and G. Comsa, *Phys. Rev. Lett.* **76**, 2366 (1996). rate at the corner
- ⁷ T. A. Witten and L. M. Sander, *Phys. Rev. Lett.* **47**, 1400 (1981).
- ⁸ T. Irisawa, M. Uwaha and Y. Saito; *Europhys. Lett.* **30**, 139 (1995).
- ⁹ G. S. Bales and D. C. Chrzan, *Phys. Rev. B* **9**, 6057 (1994).
- ¹⁰ Z. Zhang, X. Chen and M. G. Lagally, *Phys. Rev. Lett.* **73**, 1829 (1994).
- ¹¹ S. Ovevsson, A. Bogicevic, and B. I. Lundqvist, *Phys. Rev. Lett.* **83**, 2608 (1999).
- ¹² J. G. Amar, *Phys. Rev. B* **60**, R11317 (1999).
- ¹³ O. Pierre-Louis, M. R. D'Porsogna, and T. Einstein, *Phys. Rev. Lett.* **82**, 3661 (1999).
- ¹⁴ M. V. Ramana Murty and B. H. Cooper, *Phys. Rev. Lett.* **83**, 352 (1999).
- ¹⁵ J. A. Venables, *Phil. Mag.* **27**, 697 (1973).
- ¹⁶ S. Stoyanov and D. Kashchiev, in *Current Topics in Material Science*, edited by E. Kaldis (North-Holland, Amsterdam, 1981), Vol. 7, pp.69-141.
- ¹⁷ M. C. Bartelt and J. W. Evans, *Phys. Rev. B* **46**, 12675 (1992).
- ¹⁸ P. A. Mulheran and D. A. Robbie, *Phys. Rev. B* **64**, 115402 (2001).
- ¹⁹ J. Villain, A. Pimpinelli, L.-H. Tang, and D. Wolf, *J. de Physique I* **2**, 2107 (1992)
- ²⁰ L.-H. Tang, *J. de Physique I* **3**, 935 (1993)
- ²¹ F. Liu, A. H. Li, and M. G. Lagally, *Phys. Rev. Lett.* **87**, 126103 (2001).